



**ICTAM 2024**  
THE 26<sup>TH</sup> INTERNATIONAL CONGRESS OF  
THEORETICAL AND APPLIED MECHANICS

[www.ictam2024.org](http://www.ictam2024.org)

THE 26<sup>TH</sup> INTERNATIONAL CONGRESS OF  
THEORETICAL AND APPLIED MECHANICS

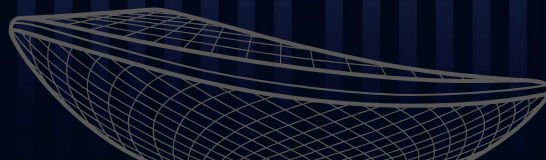
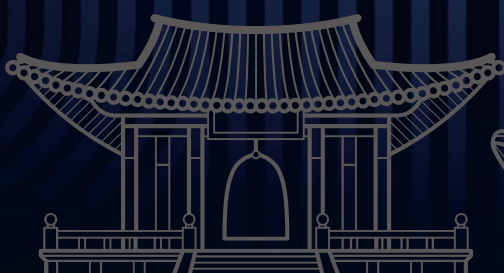
# ICTAM

## 2024 DAEGU, KOREA

25<sup>SUN</sup> – 30<sup>FRI</sup> AUGUST 2024

THE 100<sup>TH</sup> ANNIVERSARY OF ICTAM

Abstract Book



ORGANIZER



KCTAM

HOST



SPONSORS



# THE EFFECT OF PLASTIC ANISOTROPY AND TENSION COMPRESSION-ASYMMETRY ON VOID GROWTH IN DUCTILE MATERIALS WITH REALISTIC POROUS MICROSTRUCTURES

G. Vadillo<sup>1,\*</sup>, N. Hosseini<sup>1</sup>, A. R. Vishnu<sup>1</sup>, M. Dakshinamurthy<sup>1</sup>, S. Hashem-Sharifi<sup>1</sup>, J. C. Nieto-Fuentes<sup>1</sup>, K. Kowalczyk-Gajewska<sup>2</sup> & J. A. Rodríguez-Martínez<sup>1</sup>

<sup>1</sup>Department of Continuum Mechanics and Structural Analysis. University Carlos III of Madrid, Leganés, Spain

<sup>2</sup>Institute of Fundamental Technological Research, Polish Academy of Sciences, Pawińskiego 5b, 02 106 Warsaw, Poland

**Summary** We have investigated the effect of plastic anisotropy and tension-compression asymmetry on void growth from materials which contain realistic porous microstructures considering 3D unit cells and two approaches: crystal plasticity models and macroscopic models. For that purpose, we have performed finite element calculations of cubic unit-cells which are subjected to periodic boundary conditions and include porosity distributions representative of different additively manufactured metals.

## INTRODUCTION

In order to elucidate the role of real void sizes or real intervoid distances on the mechanisms of ductile fracture, finite element simulations, including distributions of voids obtained from X-ray tomography analysis of porous materials, bring about opportunities to study ductile damage in realistic situations. The main objective of our work is to analyse the effect of plastic anisotropy and tension-compression-asymmetry on void growth in ductile materials with realistic porous microstructures. The matrix material will be described considering two approaches: a crystal plasticity framework [1] and classic anisotropic formulations [2],[3] and [4]. To the authors' knowledge, an experimentally-based void configuration with a number of pores large enough to ensure a significant statistical representation of the porous microstructure was never fully mapped within a 3D representative volume element.

## CONSTITUTIVE MODELS

### Crystal plasticity model:

$$\begin{aligned} \mathbf{F} &= \mathbf{F}^e \mathbf{F}^p, & \dot{\tau}_\alpha &= h_0 \sum_{\beta=1}^{N^s} q_{\alpha\beta} \left(1 - \frac{\dot{\tau}_\beta}{\dot{\tau}_s}\right)^{p_2} |\dot{\gamma}_\beta| \\ \mathbf{F}^p &= \left( \sum_{\alpha=1}^{N^s} \dot{\gamma}_\alpha \tilde{\mathbf{M}}_\alpha \right) \mathbf{F}^p, & \tau_\alpha &= \tilde{\mathbf{T}} \tilde{\mathbf{M}}_\alpha \\ \mathbf{n}(t)_\alpha &= \left( \mathbf{F}^{eT} \right)^{-1} \tilde{\mathbf{n}}_\alpha, & \tilde{\mathbf{M}}_\alpha &= \tilde{\mathbf{m}}_\alpha \otimes \tilde{\mathbf{n}}_\alpha, \tilde{\mathbf{T}} = \left( \mathbf{F}^{eT} \mathbf{F}^e \right) \tilde{\mathbf{S}} \approx \mathbf{F}^p \mathbf{S} \mathbf{F}^{pT} \\ \dot{\gamma}_\alpha &= \dot{\gamma}_0 \left| \frac{\tau_\alpha}{\tau_s} \right|^{p_1} \text{sign}(\tau_\alpha), & \mathbf{m}(t)_\alpha &= \mathbf{F}^e \tilde{\mathbf{m}}_\alpha, \tilde{\mathbf{S}} = \frac{\partial \Psi}{\partial \mathbf{E}^e} = \mathbf{C} : \mathbf{E}^e \end{aligned}$$

### Stewart and Cazacu (2006) 's macroscopic model [5]:

$$f = \bar{\sigma} - \sigma_Y = 0 \quad \bar{\sigma} = \left( \frac{\phi_{\text{CPB06}}}{\eta} \right)^{1/a} \phi_{\text{CPB06}} = \sum_{i=1}^3 (|\tilde{s}_i| - k \tilde{s}_i^*)^a$$

$$\mathbf{L} = \begin{bmatrix} L_{11} & L_{12} & L_{13} & 0 & 0 & 0 \\ L_{12} & L_{22} & L_{23} & 0 & 0 & 0 \\ L_{13} & L_{23} & L_{33} & 0 & 0 & 0 \\ 0 & 0 & 0 & L_{44} & 0 & 0 \\ 0 & 0 & 0 & 0 & L_{55} & 0 \\ 0 & 0 & 0 & 0 & 0 & L_{66} \end{bmatrix}$$

## FINITE ELEMENT MODEL

The finite element model (see Fig. 1) used in simulations is a cubic unit-cell containing spatially distributed spherical voids of different sizes. This cell model is considered to be a representative volume element of a porous material. The equations for the nodal displacements reported in [1] have been used to impose periodic boundary conditions on the unit-cell, so that the displacement of opposed external nodes is coupled. Constant and controlled values of the macroscopic stress triaxiality and Lode parameter are prescribed during the entire loading history.

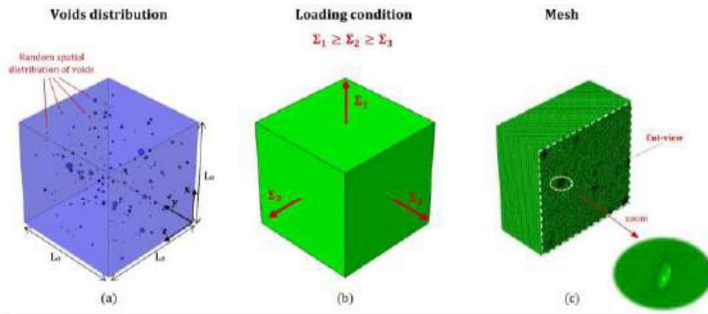


Figure 1. (a) semi-transparent view displaying the porous microstructure, (b) loading conditions with  $\Sigma_1, \Sigma_2$  and  $\Sigma_3$  being the principal values of the macroscopic stress tensor and (c) cut-view showing the fine mesh around the voids [2].

## SAMPLE RESULTS

Figure 2 presents the influence of void on the heterogeneity of lattice rotation in a soft-hard bi-crystal, at  $T = 0$  and  $L=1$ . Initially all elements within each half cell have the same orientation. It becomes apparent that while for a bi-crystal without a void, lattice rotates uniformly within each half cell, strong variation is observed when the voids are present at the grain boundary. The largest misorientation angle ( $> 45$ ) is observed close to the void boundary, where the void is distorted most.

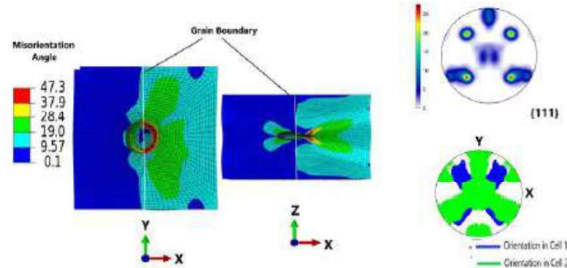


Figure 2. Distribution of misorientation angle with respect to the initial orientation for soft-hard bi-crystal for  $T = 0, L = -1$  and equivalent strain  $\bar{\epsilon} = 0.45$ . Pole figures 111 present the spread of the current crystal orientations for each Gauss point in the cell [1]

Fig. 3 shows the evolution of  $f/f_0$  with the angular misalignment  $\theta$  for  $L=-1$  and  $T=0.33, 1$  and  $2$ . Results correspond to aluminium alloy 2090-T3 for material orientations in the case of  $x \parallel \Sigma_{III}$   $y \parallel z_0$ , which means the minor loading direction  $\Sigma_{III}$  is parallel to the rolling direction  $x$ , and the transverse and normal orthotropy axes,  $y$  and  $z$ , form an angle  $\theta$  with the other two loading directions. The minimum is shallow for  $T = 0.33$ , and much stronger for  $T = 2$ , so that the nonlinearity of the  $f/f_0$ - $\theta$  curves become more important as the triaxiality increases, bringing out the interplay between angular misalignment and stress triaxiality on void growth. The angle  $\theta$  for which the minimum occurs, while hardly dependent on the value of  $T$ , depends strongly on the material orientation.

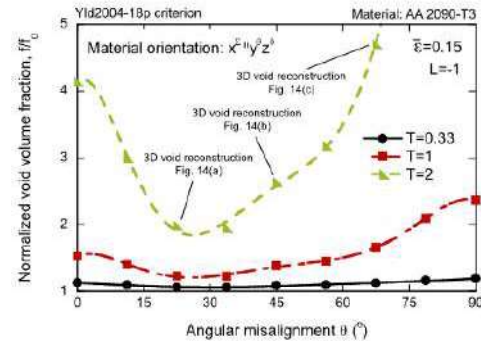


Fig.3. Influence of the macroscopic stress triaxiality on void growth for AA 2090-T3. Unit-cell finite element calculations for  $L = -1$  and  $T = 0.33, 1$  and  $2$ . Evolution of the normalized void volume fraction  $f/f_0$  with the angular misalignment  $\theta$  and material orientation  $x \parallel \Sigma_{III}$   $y \parallel z_0$  [3]

Fig. 4 presents contours of effective plastic strain for a porous microstructure with 27 voids and 5 clusters. The cluster contains voids which grow and rapidly interact with each other shortly after the loading starts, such that most of the pores are no longer spherical for  $\bar{\epsilon} = 0.033$ , with the voids surrounding the largest pores displaying a mushroom shape with a flattened face corresponding to the formation of an intervoid ligament. The flattening of the voids generally starts earlier than in the case of the porous microstructures with randomly distributed voids since packing the voids into clusters decreases the distance between voids. For  $\bar{\epsilon} = 0.066$  the plastic strain in the surface of most pores is greater than 1, and the separation between voids is minimal, depicting the beginning of coalescence.

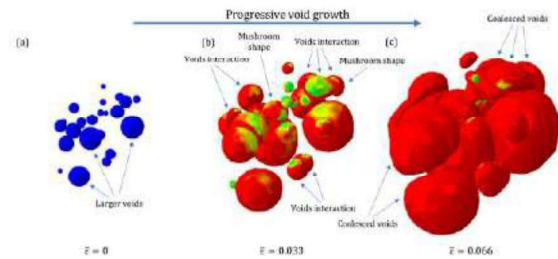


Figure 4. Results corresponding to porous microstructure with 27 voids and 5 clusters. Stress triaxiality  $T = 3$  and Lode parameter  $L = -1$ . Snapshots corresponding to different values of macroscopic effective strain: (a)  $\bar{\epsilon} = 0$ , (b)  $\bar{\epsilon} = 0.033$  and (c)  $\bar{\epsilon} = 0.066$  [4].

## SUMMARY AND CONCLUSIONS

We have carried out a comprehensive numerical investigation on the role of real porous microstructure on the ductile behavior of 3D printed metals. The matrix material was described considering two approaches: a crystal plasticity framework and classic anisotropic formulations. The simulations have been carried out with random spatial distributions of voids and with clusters of the same size but different void densities, and the results have been compared to unit-cells with a single central pore. Calculations exchanging the loading directions for a given distribution of void sizes and positions have been performed to elucidate whether the evolution of the porous microstructure leads to anisotropic behavior of the unit-cell.

## ACKNOWLEDGEMENTS

The financial support provided by the Spanish Ministry of Science and Innovation under the programme Proyectos I+D Excelencia 2017 is kindly acknowledged. Project APPLIED, DPI2017-88608-P.

This work was supported by the European Union's Horizon Europe Programme (Excellent Science, Marie-Sklodowska-Curie Actions) under REA grant agreement 101086342 (Project DIAGONAL)

The research leading to these results reported has received funding from the European Research Council under the European Union's Horizon 2020 research and innovation programme. Project PURPOSE, grant agreement 758056.

## References

- [1] Dakshinamurthy, M., Kowalczyk-Gajewska, K., Vadillo, G. Influence of crystallographic orientation on the void growth at the grain boundaries in b-crystals. *International Journal of Solids and Structures*. 2021, 212, 61–79.
- [2] Hashem-Sharifi, S., Hosseini, N., Vadillo, G. 3D numerical simulations and microstructural modeling of anisotropic and tension–compression asymmetric ductile materials. *International Journal of Solids and Structures*. 2022, 256, 111936.
- [3] Hosseini, N., Nieto-Fuentes, J. C., Dakshinamurthy, M., Rodríguez-Martínez, J.A., Vadillo, G. The effect of material orientation on void growth. *International Journal of Plasticity*. 2022, 148, 103149.
- [4] Vishnu, A. R., Vadillo, G., Rodríguez-Martínez, J. A. Void growth in ductile materials with realistic porous microstructures. *International Journal of Plasticity*, 2023, 167, 103655.
- [5] Cazacu O., Plunkett B., Barlat F. Orthotropic yield criterion for hexagonal closed packed metals. *International Journal of Plasticity*. 2006, 22, 1171-1194